Determination of Cloud Liquid Water Distribution by Inversion of Radiometric Data

J. WARNER AND J. F. DRAKE

National Center for Atmospheric Research, Boulder, CO 80307*

P. R. KREHBIEL

New Mexico Institute of Mining and Technology, Socorro, NM 87801

(Manuscript received 27 June 1984, in final form 23 January 1985)

ABSTRACT

A method is described whereby the distribution of liquid water through a cross section of a cloud may be determined from radiometric data. It involves the scanning of the cloud by a pair of ground-based centimeter wave radiometers and measuring the emission from a multiplicity of different directions. The time required to obtain all of the necessary information should be less than three minutes. The emission is sensibly independent of the presence of ice in the cloud and depends essentially upon the integrated liquid water content along the path. Corrections need to be made for the mean temperature and water vapor profiles in the cloud and the clear air environment. If there is significant water content in drops larger than about 1 mm diameter the emissivity becomes drop size dependent, so the technique is useful only in the preprecipitation phase of cloud development or before the rain rate reaches about 1 mm h^{-1}. The distribution of liquid water is determined by mathematical inversion procedures. Simulation studies suggest that the technique should be capable of yielding the liquid water content to within about 10% of the maximum water content within the cloud with a spatial resolution of a few hundred meters.

1. Introduction

Until recently the distribution of liquid water in clouds has been measured only from instrumented research aircraft. A wide variety of techniques has been used to determine water content; for example, it has been deduced from measurements of the power required to evaporate the water impacted on a heated wire or from measurements of the light scattered or obscured by droplets in a laser beam. These techniques are usually designed to be of fast response and enable the detailed structure of the cloud to be examined. However, unless many aircraft are used for simultaneously traversing the cloud at different levels, only a small part of the cloud can be sampled at one time. A single aircraft is likely to take upwards of 20 min to make enough traverses through a cloud to obtain a reasonable estimate of the distribution of cloud water; during this time considerable changes in the structure of the cloud are likely.

The present paper describes a remote sensing technique whereby a complete vertical cross section of the distribution of cloud water can be obtained from data taken in two or three minutes. The method involves measurement of microwave emission from the cloud in many different directions and mathematical inversion of this data to obtain liquid water distribution. It is a computed tomographic method that is similar in principle to the various imaging techniques, now being used in medical and other fields, which measure absorption or emission for a number of projections at different angles and use the measurements to reconstruct cross-sectional images (e.g., Herman, 1980). The scanning technique is different because of practical considerations involved in scanning a cloud, and the inversion technique has been developed to suit this particular problem.

A somewhat different application of microwave radiometry using tomographic methods was proposed by Shaari and Hodge (1978) to determine the location and intensity of rain cells. However, the method they employed did not give satisfactory results when they simulated storm detection using only two radiometers and they did not consider the possibility of determining cloud water distribution.

2. Radiometric considerations

In passing through cloud or precipitation, whether the particles are in liquid or solid form, microwave radiation is attenuated either by scattering or absorption. For droplets that are small in comparison to the wavelength, the attenuation is almost entirely due to absorption and is directly proportional to the total volume of the drops per unit volume of the atmosphere,

* The National Center for Atmospheric Research is sponsored by the National Science Foundation.

i.e., the liquid water content. At a wavelength of 1 cm the absorption is approximately 1 dB km^{-1} per g m^{-3} of liquid water. The absorption varies slightly with the temperature of the droplets, increasing by about 3% for 1°C decrease in temperature at 0°C. Ice absorbs a negligible amount of radiation at centimeter wavelengths and its concentration is so low that scattering of natural radiation is insignificant. Hence attenuation through a mixed phase cloud is due to the liquid water present, not to the total condensed water. The importance of large droplets and of ice particles that develop a wet surface as they fall through the 0°C level will be discussed later, together with other limitations in the proposed technique.

Since the cloud absorbs microwave energy it will also emit, and Kirchhoff's law implies that the emissivity equals the absorptivity. The emission from a unit volume depends in part upon the number of drops in that volume, i.e., the liquid water content, and their temperature. Viewed from outside the cloud, the radiation received from a particular direction will be the sum of the input at the far side of the cloud, as diminished by absorption while traversing the cloud, and the emission of all the elements of liquid water as modified by absorption along the path. In order for emission measurements to be useful, they must be made at a frequency where the emission can be accurately measured but is not so strong that the signal from the far side of the cloud is markedly attenuated. These conditions are satisfied at centimeter wavelengths with nonprecipitating clouds, and then one cannot ignore the radiation incident on the far side of the cloud. When viewed from below, as we propose, the incident radiation is the (constant) cosmic background and radiation from atmospheric gases above the cloud top. Attempts to observe from above would be complicated by the (unknown) temperature and variable emissivity of the earth's surface.

By suitable choice of frequency in the 1 cm band it is possible to operate in a transmission "window," as far as water vapor is concerned. However, even though its absorption and emission are then low, they are not negligible in comparison to the effect of liquid water: hence, allowance must be made for them in the computations. In addition the absorption and emission of oxygen must be considered. The effect of other atmospheric gases can be neglected. Thus in drawing inferences from the emission from a cloud in a given direction we must take into account the cosmic background, the emission and absorption of the liquid water and the emission and absorption of water vapor and oxygen. Whilst water vapor has an absorption coefficient dependent upon both pressure and temperature its main importance lies in its concentration. Within the cloud the concentration is directly related to the temperature, since the air is very close to saturation except possibly in extreme updrafts or when precipitation is well-developed. As will be shown later a knowledge of the temperature and water vapor vertical profiles to about 1°C and 1 g kg^{-1} is sufficient.

3. Equipment configurations

Three possible configurations have been considered—two ground-based, and the other airborne; they are shown schematically in Fig. 1. The first involves absorption between an airborne transmitter and an array of receivers on the ground. We have decided not to attempt this approach for several reasons, including the cost of deploying the receiving and recording array and problems associated with transmitter and receiver antenna patterns. The aircraft would need to be accurately tracked and one would be restricted to studying clouds over the array. However, the approach has the advantage of providing reconstructions that are potentially more accurate (because of the increased number of measurements), in shorter time and simultaneously in more than one plane.

Both of the other systems are based on emission from the cloud under study: in the first case, ground-based scanning radiometers measure the radiation from a large number of intersecting paths through the cloud whilst in the second, two fixed antennas on an aircraft scan the cloud in a series of intersecting paths as the aircraft flies below cloud base. In both configurations the signals received from the direction of each ray contain information about the liquid water along that ray. The distribution of water within the whole plane scanned can be obtained by the following mathematical inversion method. By scanning in planes off the zenith as well as through it, it should be possible (at least in principle) to obtain three-dimensional information regarding the distribution of liquid water throughout the cloud.

In order to investigate the accuracy with which it should be possible to retrieve the cloud water distribution from radiometric data a series of numerical simulations has been carried out, the results of which are described herein. Most work has been done on the configuration involving two ground-based scanning radiometers since such radiometers were available for field trials. The results of these trials will be reported separately. Sufficient work has been done in simulating the airborne system to indicate that its behavior is generally similar to that of the ground-based system. The airborne configuration is probably preferred, in that it enables measurements to be made anywhere and is not dependent upon clouds forming or moving over a fixed ground site; however, much more work needs to be done and the results will be reported later.

Any practical radiometer will have a certain antenna pattern and receiver sensitivity. The latter is limited by random noise and is commonly expressed as a minimum change in brightness temperature that can be detected. In what follows we will call this the receiver noise level. The radiometer characteristics used in the

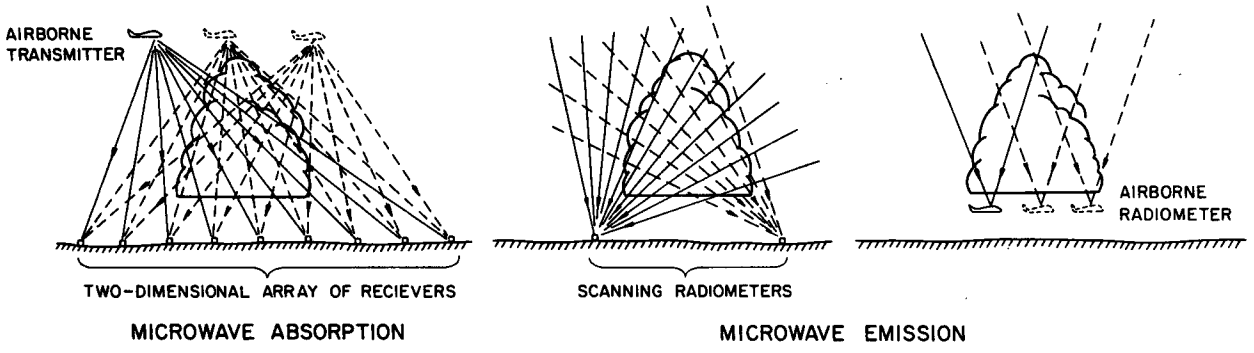

FIG. 1. Equipment configuration for the collection of radiometric data necessary to calculate the distribution of liquid water content in a cloud.

simulations described below were based on those of the steerable dual-channel microwave radiometer described by Hogg *et al.* (1983). Indeed, two of these radiometers were made available by NOAA's Wave Propagation Laboratory for the field trials to be described elsewhere.

4. Mathematical inversion techniques

The liquid water density ρ_l produces its effect on the observed radiation through the coefficient of absorption per unit path length α,

$$\alpha = \alpha_{02} + \kappa_l \rho_l + \alpha_v, \tag{1}$$

where α_{02} is the absorption per unit length due to molecular oxygen, α_v that due to water vapor and κ_l is the mass density absorption coefficient for liquid water.

The formulae used for α_v and κ_l were those of Westwater (1972) but for α_{02} that of Falcone (1966) was used since Westwater's formula for oxygen is more complicated than necessary for the frequency of interest here (31.6 GHz). The formulae are given in the Appendix.

An important quantity depending on α that enters the equation of radiative transfer is $\tau(\theta, l_1, l_2)$, the transmission between two points at distances l_1 and l_2 from a radiometer, measured along a ray leaving at an angle θ from the line connecting the two radiometers ($l_1 \leqslant l_2$).

$$\tau(\theta, l_1, l_2) = \exp\left\{-\int_{l_1}^{l_2} \alpha[\mathbf{r}(\theta, s)]ds\right\}, \tag{2}$$

where $\mathbf{r}(\theta, s)$ is the point a distance s along the ray at angle θ. This is sufficient to define the position because all rays lie in the vertical plane containing the radiometers.

The equation of radiative transfer (without scattering) for these simulations may now be written as

$$I(\theta) = I_\infty \tau(\theta, 0, z_t \csc\theta) + \int_0^{z_t \csc\theta} B[T(\mathbf{r})]\alpha(\mathbf{r})\tau(\theta, 0, s)ds, \tag{3}$$

where $I(\theta)$ is the radiance of the radiation reaching a radiometer from the pencil at angle θ; I_∞ the specific intensity of the cosmic background radiation, taken to be isotropic; z_t the depth of the atmosphere containing radiatively significant constituents; s the path length along the ray at angle θ; and $B(T)$ is the Planck function at 31.65 GHz and temperature T.

It should be noted that in the retrieval of atmospheric temperature from radiometric data, α and τ are assumed to be known (at least approximately) in order to infer the spatial distribution of the Planck function B, or equivalently of T. However, in the retrieval of liquid water content the opposite procedure is followed. It may also be of interest to note that the fractional change of B with temperature at centimeter wavelengths is an order of magnitude less than it is in the infrared, which implies that in our case the principal source of difference between one measurement and another is the variation in the amount of absorbing material present.

a. Synthesis of the data for the simulations

The state of the simulated atmosphere, including the location and properties of the simulated cloud, are specified by giving ρ_v, the water vapor density, ρ_l, and T as functions of position. In the cloud, ρ_v takes on its saturated value. The directions of the beams that each radiometer is to measure are then used with a specified beam width to determine the angles for which I must be computed. Beam intensity is computed as the integral over the beam of pencil intensities weighted by the pattern of antenna gain which, with unit total weight may be written as

$$\left(\frac{4 \ln 2}{\pi w^2}\right)^{1/2} \exp[-(4 \ln 2)(\xi/w)^2] \tag{4}$$

where ξ is the angular separation of a ray from the antenna axis and w is the width of the antenna beam between rays where the gain is half its maximum value. The four-point Gauss-Hermite quadrature formula

with weights w_k and abscissae ξ_k is used, giving for the intensity of the ith beam

$$\bar{I}(\theta_i) = \sum_{k=1}^{4} w_k I(\theta_{ik}). \tag{5}$$

where $\theta_{ik} = \theta_i + \xi_k$. The true beam intensities are perturbed randomly to simulate the effect of instrumental noise. Because the receiver sensitivity is given in terms of a minimum detectable change in brightness temperature the following formula is used for the simulated beam intensity, $\tilde{I}(\theta_i)$:

$$\tilde{I}(\theta_i) = B\{B^{-1}[I(\theta_i)] + X\sigma_b\}, \tag{6}$$

where X is a Gaussian random variable with zero mean and unit standard deviation and σ_b is the accuracy of the radiometer in K.

b. Inverting the radiometric data to obtain ρ_l

The simulated beam intensities are approximately equal to the true beam intensities:

$$\bar{I}(\theta_i) \approx \tilde{I}(\theta_i), \quad i = 1, 2, 3, \ldots, m. \tag{7}$$

Expanding $\bar{I}$ using (3) and (5) gives

$$\sum_{k=1}^{4} w_k \Bigg[I_\infty \tau(\theta_{ik}, 0, z_t \csc\theta_{ik}) + \int_0^{s_1} B\alpha\tau ds + \int_{s_1}^{s_2} B\alpha\tau ds + \int_{s_2}^{z_t \csc\theta_{ik}} B\alpha\tau ds \Bigg] \approx \tilde{I}(\theta_i), \quad i = 1, 2, 3, \ldots, m \tag{8}$$

where s_1 and s_2 are the path lengths at which the ray with direction θ_{ik} enters and leaves the cloud. If the ray designated by (i, k) misses the cloud entirely, as will happen for some beams just grazing the cloud, the generalization is obvious from what follows.

Using the property of τ that

$$\tau(\theta, l_1, l_3) = \tau(\theta, l_1, l_2)\tau(\theta, l_2, l_3), \quad \text{where} \quad l_1 \leqslant l_2 \leqslant l_3, \tag{9}$$

(8) may be rewritten as

$$\sum_{k=1}^{4} \tau(\theta_{ik}, 0, s_1) \int_{s_1}^{s_2} B\alpha\tau(\theta_{ik}, s_1, s) ds \approx \tilde{I}(\theta_i) - \sum_{k=1}^{4} w_k \Bigg[\int_0^{s_1} B\alpha\tau(\theta_{ik}, 0, s) ds + \tau(\theta_{ik}, 0, s_2)\underline{\tau(\theta_{ik}, s_1, s_2)} \int_{s_2}^{z_t \csc\theta_{ik}} B\alpha\tau(\theta_{ik}, s_2, s) ds + \underline{\tau(\theta_{ik}, 0, z_t \csc\theta_{ik})} I_\infty \Bigg], \quad i = 1, 2, 3, \ldots, m. \tag{10}$$

In this equation the only explicit dependence on α within the cloud, and thus on ρ_l, is the appearance of α in the integrals on the left side, though there is a hidden dependence through the underlined transmission factors.

In the mathematical reconstruction of α within the cloud, and then ρ_l, the *true distributions* of T and ρ_v are not among what is given, but it is assumed that the horizontal mean of T and ρ_v outside the cloud and that of T within the cloud are known; these means are used when needed to estimate quantities such as $\tau(\theta_{ik}, 0, s_1)$, the transmission between radiometer and cloud, appearing in (10). The reconstructed cloud is taken to be saturated at the horizontal mean temperature for each elevation.

If the underlined factors can be estimated, then (10) is a system of m coupled linear integral equations for the unknown α within the cloud. If this system may be solved then the result can be used to improve the estimates of the underlined quantities, and a better α within the cloud computed in the usual procedure of approximation by successive substitution.

These equations are discretized by assuming that in the cloud

$$\alpha(\mathbf{r}) = \sum_{j=1}^{n} \alpha_j \phi_j(\mathbf{r}), \tag{11}$$

where the α_j are coefficients in a Galerkin approximation in which each basis function ϕ_j is nonzero only in the jth small square within the cloud, and there $\phi_j = 1$. The cloud was divided into n such elements of equal size, where $n = N^2$ for some integer N. With this assumption, Eq. (10) becomes

$$A\boldsymbol{\alpha} \approx \mathbf{b}, \tag{12}$$

where $A = (a_{ij})$ is an $m \times n$ matrix, $\boldsymbol{\alpha}^T = (\alpha_1, \alpha_2, \alpha_3, \ldots, \alpha_n)$, and $\mathbf{b}^T = (b_1, b_2, b_3, \ldots, b_m)$ with

$$a_{ij} = \sum_{k=1}^{4} w_k \tau(\theta_{ik}, 0, s_1) \int_{s_1}^{s_2} B\phi_j(\mathbf{r})\tau(\theta_{ik}, s_1, s) ds \tag{13}$$

and b_i is equal to the right side of the ith equation in (10). In the simulations to be described $m > n$ and Eq. (12) was solved as a linear least squares problem in which the components of the solution vector were constrained to be nonnegative using the algorithms NNLS (Lawson and Hanson, 1974) and LSEI (Hanson and Haskell, 1982).

A combination of mesh refinement and successive approximation was used to build the resolution up to $N \times N$ cells. First, an estimate of α within the cloud was made from the synthetic data with the cloud taken to be homogeneous, α_0, and it was used as the first approximation for a calculation with 2×2 resolution, α_1. Successive substitution was performed at this resolution until α_1 converged; then α_1 was used as a first approximation in the iterations at 4×4 resolution that yield α_2, and so on up to $n \times n$ resolution, except that for resolutions $2^j \times 2^j$ with $1 < j < \log_2 n$ only one iteration of successive substitution was done. 20 iter-

ations were done with $N \times N$ cells and from among the successive approximate solutions at this resolution the one giving the residual vector $A\alpha - \mathbf{b}$ of least length was taken to be the best estimate of the true α.

5. Results of some simulations

Only a few of the many simulations that have been carried out will be reported here. In most cases it has been assumed that the "cloud" consists of a central core of high liquid water content surrounded by rings of uniform but decreasing water content toward the cloud edge. We have called this an "onion" distribution. However, a sufficient number of simulations have been carried out for a random distribution of liquid water (a "diced onion" distribution) to ensure that the technique is equally successful in its ability to reconstruct the original liquid water field. In order to keep computational time within reasonable limits for the large number of simulations undertaken, the size of the array of elements used to simulate a cloud was restricted typically to 10×10 or 8×8. One simulation for an 8×8 array takes 10 sec of CRAY 1 computer time. The "cloud" was usually assumed to be 5 km $\times$ 5 km in size and to be midway between two scanning radiometers 10 km apart and to have its base at a height of 2.5 km above the surface.

In the initial simulations the presence of water vapor was neglected and it was assumed that the radiometric information came from a series of rays equally spaced in angle, all of which intersected the cloud. An example of an original field showing an onion distribution and one reconstruction of it is given in Table 1. A similar example for the "diced onion" distribution is given in Table 2. In both cases the radiometer receiver noise level has been assumed to be 0.2 K and the total number of rays to be 120 (shared equally between the two radiometers). Since the receiver noise is a random function differing from ray to ray and simulation to simulation each reconstruction differs from its predecessor. In what follows the average of nine reconstructions was usually taken to represent the total population. Nine is too small a number to make the deviations from the population means negligible, but was chosen to limit computational time: as a result there is scatter in the resulting plots of rms errors in the reconstructed field versus number of rays.

TABLE 1. Typical realization for "onion" distribution with $\rho_{l_{max}} = 1.5$ g m^{-3} and $n = 10$, number of rays = 120, $\sigma_N = 0.2$ K.

true ρ_l									
0.30	0.30	0.30	0.30	0.30	0.30	0.30	0.30	0.30	0.30
0.30	0.60	0.60	0.60	0.60	0.60	0.60	0.60	0.60	0.30
0.30	0.60	0.90	0.90	0.90	0.90	0.90	0.90	0.60	0.30
0.30	0.60	0.90	1.20	1.20	1.20	1.20	0.90	0.60	0.30
0.30	0.60	0.90	1.20	1.50	1.50	1.20	0.90	0.60	0.30
0.30	0.60	0.90	1.20	1.50	1.50	1.20	0.90	0.60	0.30
0.30	0.60	0.90	1.20	1.20	1.20	1.20	0.90	0.60	0.30
0.30	0.60	0.90	0.90	0.90	0.90	0.90	0.90	0.60	0.30
0.30	0.60	0.60	0.60	0.60	0.60	0.60	0.60	0.60	0.30
0.30	0.30	0.30	0.30	0.30	0.30	0.30	0.30	0.30	0.30
inferred ρ_l − true ρ_l; rms error = 0.042 g m^{-3}									
0.00	0.00	0.00	−0.03	−0.04	−0.06	−0.01	−0.01	−0.01	0.01
0.01	0.03	0.03	−0.01	0.02	0.03	0.03	0.13	0.00	0.02
0.01	0.06	−0.05	−0.01	0.01	−0.08	−0.12	0.03	0.00	−0.06
0.05	0.06	0.00	0.06	0.07	−0.08	−0.01	0.02	0.05	−0.01
−0.03	−0.04	−0.01	0.05	0.03	−0.10	0.02	0.02	0.10	0.05
−0.01	−0.03	−0.03	0.07	0.03	−0.04	0.02	−0.05	0.06	−0.01
−0.04	−0.03	0.01	0.02	−0.05	−0.05	0.02	−0.07	0.07	0.01
−0.01	−0.03	0.01	−0.02	−0.03	−0.05	0.03	−0.06	0.05	0.00
0.00	0.03	0.04	−0.02	0.00	−0.04	−0.03	−0.09	0.00	0.01
0.00	0.02	0.04	0.02	0.04	0.01	−0.03	−0.04	−0.01	0.00

TABLE 2. Typical realization for "diced onion" distribution with $\rho_{l_{max}} = 1.5$ g m^{-3} and $n = 10$, number of rays = 120, $\sigma_N = 0.2$°K.

true ρ_l									
0.36	0.95	0.05	0.69	0.09	0.06	0.58	0.24	1.09	0.32
0.04	0.13	0.81	0.35	0.48	0.81	1.04	0.23	0.36	0.15
0.17	0.35	0.96	0.07	0.31	0.13	0.66	0.30	0.07	0.94
0.68	1.03	0.11	0.09	0.50	0.01	0.28	1.31	0.37	0.42
0.49	0.71	0.14	0.44	0.49	0.12	0.29	1.10	0.98	0.31
1.38	0.32	0.40	0.56	0.77	0.27	0.43	0.03	0.17	0.21
0.71	1.07	1.29	0.10	0.19	0.06	0.86	0.52	0.35	0.24
0.67	0.01	0.66	0.05	0.35	0.60	0.57	0.57	0.71	0.43
0.25	0.02	0.19	0.34	0.50	0.75	0.99	0.33	0.49	0.20
0.57	0.25	0.04	0.81	0.44	0.70	0.12	0.08	0.78	0.38
inferred ρ_l − true ρ_l; rms error = 0.092 g m^{-3}									
0.00	0.00	−0.01	−0.01	−0.01	0.05	0.05	0.00	−0.01	0.00
0.02	0.01	0.01	0.11	0.03	−0.04	−0.09	−0.04	−0.05	−0.01
0.01	−0.14	−0.06	0.04	−0.10	−0.05	−0.21	−0.07	0.08	−0.01
0.01	−0.13	0.08	0.29	0.04	0.19	−0.19	−0.07	0.21	0.08
0.02	−0.11	−0.03	0.21	0.08	0.07	−0.08	−0.02	0.21	0.10
0.01	−0.05	0.01	0.09	−0.05	−0.06	−0.14	−0.03	0.19	0.03
−0.02	0.00	0.17	0.25	0.17	0.08	−0.04	−0.05	0.11	−0.01
−0.02	−0.01	0.01	0.03	0.03	−0.04	−0.08	−0.24	−0.03	−0.02
0.02	0.02	−0.01	−0.08	−0.06	−0.14	−0.17	−0.18	0.01	0.01
0.00	0.02	0.08	0.02	0.00	−0.05	0.01	−0.01	0.01	−0.01

The way in which the number of rays and receiver noise level affects the errors in the reconstructed field is shown in Fig. 2 for a 10×10 array having an onion distribution with a maximum liquid water content of 1 g m^{-3}. Similar calculations for different maximum liquid water contents allowed us to find the following expression for the rms errors in the reconstructed field for a 10×10 array of elements in an onion distribution being scanned by two radiometers having zero antenna beamwidth and assuming no effect of water vapor:

$$\text{rms error} = 0.1032 + 0.3011 \times (\text{receiver noise } K) - 0.03513 \times \ln(\text{number of rays} - 100) + 0.0382 \times (\text{max water content}).$$

The difference between the rms error for infinitesimal rays and 2.5° beams (simulated as described in the previous section of this paper) is shown in Fig. 3.

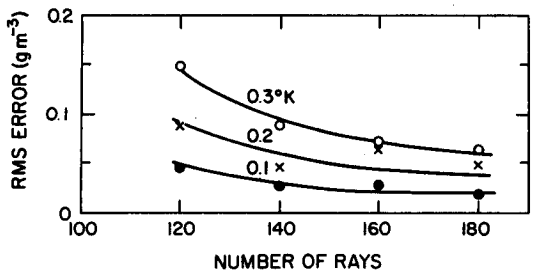

FIG. 2. Errors in the reconstructed field as a function of the receiver noise level and the number of rays for a liquid-only cloud having a central maximum liquid water content of 1 g m^{-3}.

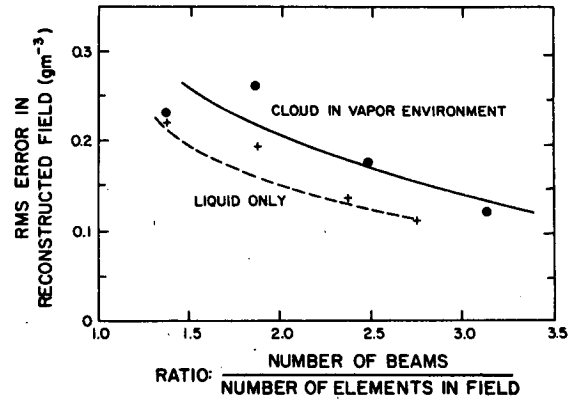

FIG. 4. Change in errors in the reconstructed field resulting from the surrounding air which was assumed to have fluctuations of temperature and water vapor content superimposed on the mean field. The cloud had a maximum liquid water content of 2.5 g m^{-3} and the radiometers had 2.5 deg beams and a noise level of 0.2 K.

Since 8 × 8 arrays as well as 10 × 10 arrays were used in producing the information used in this figure the number of rays or beams has been normalized by the number of elements in the array. Figure 4 shows the change in the effect on the error in the reconstructed field resulting from emission from the air surrounding the cloud. The air was assumed to have small fluctuations in temperature and vapor superimposed on the mean vertical profile. These fluctuations were randomly distributed at each horizontal level and were of dimension 400 m. Scales of 200 and 1000 m were also investigated but made little difference in the rms error from that with fluctuations of 400 m size. As would be expected, the error is larger for beams than for rays and if the "cloud" is contained in a nonuniform vapor field rather than in uniform dry air. The error decreases as the number of rays or beams increases but tends toward some minimum value which depends upon the maximum liquid water content in the simulated cloud and, as we shall see shortly, upon the noise level.

In Fig. 5 we see the variation in rms error with receiver noise level and number of beams for a cloud having an onion distribution with a central maximum of 2.5 g m^{-3} in a vapor field containing temperature and mixing ratio fluctuations. From this it can be seen that an increase in receiver noise level can be compensated by an increase in the ratio of beams to elements to give the same rms error in the reconstructed liquid water field. For a given total scanning time the number of beams increases as the time spent at each angle decreases and hence as the time available for integration of the incoming signal decreases. The noise level increases inversely with the square root of the integration time. As an example consider a receiver which has a noise level of 0.2 K for an integration time of 1 sec (a conservative estimate of the performance of the WPL/NOAA equipment). Reducing the integration time to 0.75 sec will increase the noise level to 0.23 K but simultaneously allow us to increase the number of

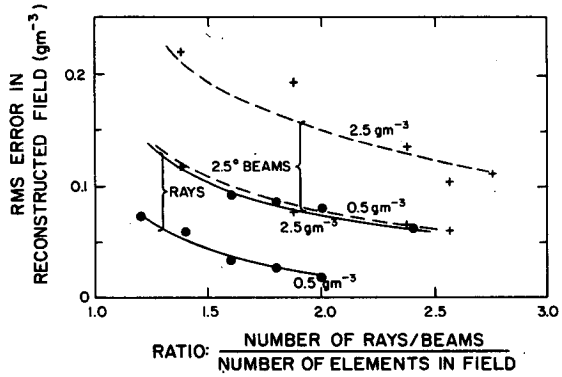

FIG. 3. Errors in the reconstructed field for radiometers having a 0.2 K noise level as a function of liquid water content and the number of rays or beams per element.

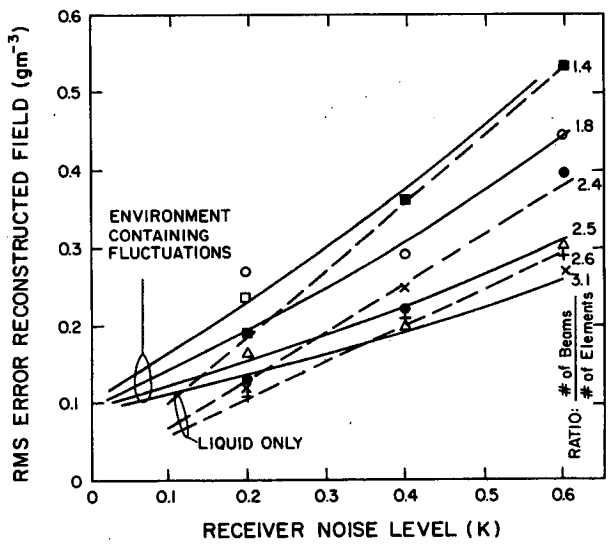

FIG. 5. Errors in the reconstructed field for a 2.5 g m^{-3} cloud as a function of receiver noise level and the number of radiometer beams per element.

beams by one third. Thus if we initially had a ratio of beams to elements of 1.9 and a noise level of 0.2 K, Fig. 5 suggests that we could increase these values to 2.4 and 0.23 respectively and yet obtain a reduction in rms errors in the reconstructed field. Since the number of beams also determines the spatial resolution that can be achieved there could be merit in increasing their number to a much greater degree while keeping the same rms error at the expense of a much greater receiver noise level. A practical limit will be reached, however, when the number of measurement beams per beamwidth of the antenna becomes very large.

Also shown in Fig. 5 are the results for a liquid-only cloud (no vapor in the environment). It is clear that at low receiver noise levels the fluctuations in the environment dominate the errors in the reconstructed field, whereas at high receiver noise levels, it is the receiver characteristics that begin to dominate—this is not, of course, an unexpected result.

A group of simulations was performed for atmospheric conditions representative of those during the summer in eastern Colorado when nonprecipitating cumuli form. The vertical profiles of the horizontal average of the environmental temperature and mixing ratio are shown in Fig. 6. As discussed in Section 4, the simulated clouds were saturated and the horizontal in-cloud average temperature was equal to the environmental mean at the same level. The magnitudes of the fluctuations from the horizontal means are given in Table 3.

The cloud was bounded by a square with 4 km sides located 2 km above the surface and centered between

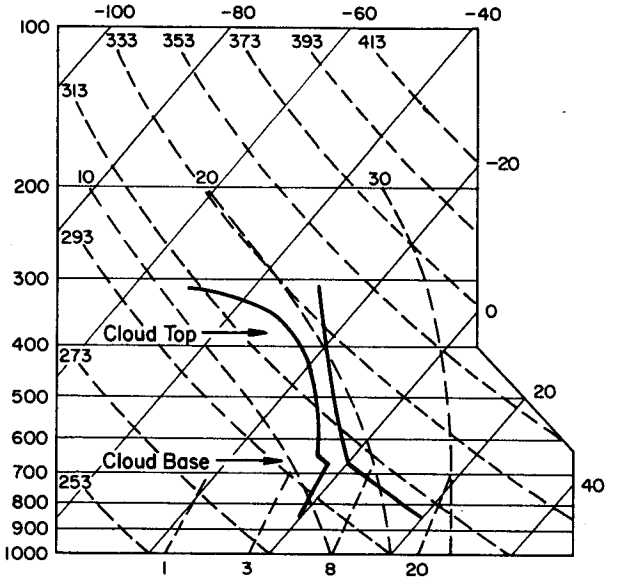

FIG. 6. Environmental sounding for an eastern Colorado summer day with nonprecipitating cumuli used for the simulations producing the results shown in Fig. 7 and Table 4.

TABLE 3. Standard deviations of fluctuations at z (km) above the surface.

	Subcloud layer (0–2 km)	Cloud environment (2–8 km)	Cloud (2–6 km)
T (K)	1	$1-(z-2)/8$	$1-(z-2)/8$
ρ_v (g m^{-3})	1	$0.5-(z-2)/16$	Dependent on T fluctuations through the saturation condition

the two radiometers, which were 8 km apart. The beam width at the half-power points of their antenna pattern was 2.5 deg. The distribution of liquid within the cloud had a broad central maximum that extended toward the lower left but was otherwise irregular. The results of retrievals made with 88 and 240 beams are summarized in Table 4. The original field for set B is shown in Fig. 7 along with the retrieved field for the realization with median rms error and the error field.

The quantitative agreement of this retrieval with the true field is good, although in some parts of the cloud the gradient in the retrieval may be twice as large as, or rotated 45 deg from, the true gradient. The contours of the error field are predominantly horizontal and those of the other realizations of this set are typically either horizontal or vertical instead of, say, diagonal or completely random. We believe this to be due to the pattern of beams for this configuration rather than to the distribution of liquid.

In all the simulations described above the position of the cloud has been assumed to be known and the beams have all been located within the cloud. In a real situation the cloud position could be unknown (though cloud base height might well be available from soundings or aircraft observations) and the only information available could be microwave emission as a function of angle. The last simulation to be described parallels this situation in that the "cloud" was in an undefined area between two radiometers which scanned from the zenith to the surface through an angle of 90 deg. The input to the inversion process was given by the calculated emission from each of 256 square elements, 500 m on a side, only 64 of which contained liquid water; the others contained water vapor and oxygen only. Fluctuations of temperature and vapor mixing ratio with the same statistics as given above were assumed to be present superimposed on the mean profiles. The total number of beams was 712.

The results of the simulation are shown in Table 5. The cloud is well located by the reconstruction process and the rms error in the area of the real cloud is only 0.09 g m^{-3}. However, the reconstruction indicates liquid water of up to 0.17 above the cloud and lesser

TABLE 4. Summary of resolution tests with eastern Colorado soundings. The number of realizations is given in parentheses after the average rms error.

Sample set	Number of cells n	Number of beams m	m/n	Average rms error (g m^{-3})	$\rho_{l_{max}}$ (g m^{-3})	Relative error (Col. 5) / (Col. 6)
A	8 × 8	88	1.38	0.22 (9)	2.53	0.09
B	8 × 8	240	3.75	0.09 (11)	2.44	0.04

amounts in other regions that were in reality cloud-free. Nevertheless, the rms error averaged over the whole field is only 0.05 g m^{-3}. Only one simulation of this type has yet been carried out but this result differs little from those in which the cloud position was known.

6. Discussion of limitations

Clearly, the proposed technique is only likely to be successful if both radiometers scan through the same emitting regions. Thus if the scan is to be limited from 0 to 90 deg it would be possible for one radiometer to see clouds on the far side of the radiometer distant from it which the latter would not look at. Some useful information may still be obtainable even in this situation by making assumptions about what is outside the field of view, but clearly the accuracy of retrieval of liquid water distribution will go down.

For the technique to be strictly applicable there should be no changes in the distribution of liquid water during the time required for the radiometers to scan through their complete field of view; that is, there should be no significant development or advection of the cloud during this period. In principle it may be possible during the computational process to make some compensation for advection but this would demand a knowledge of cloud motion at all levels and could be a difficult task. Hence, it is obviously desirable to complete the scanning process as rapidly as possible. This implies that only short time periods are available for integration of the received signal with consequent increases in receiver noise level. As mentioned earlier there is a trade-off between receiver noise level and the number of beams, and in general it appears desirable to accept some degradation in receiver performance in order to increase the number of beams and yet keep the total scanning period reasonably short. Exactly what should be done in practice would depend upon the degree to which the cloud could be regarded as being nonvarying (which determines the total time available for scanning), the spatial resolution required and the errors in the reconstructed field which can be tolerated; the last two quantities are affected by the number of beams employed and the receiver integration time.

As was mentioned earlier in this paper, microwave absorption or emission is directly proportional to liquid water content and independent of the size distribution of the droplets provided the latter are small in comparison to the wavelength. Exactly how this limits the proposed technique, which employs a wavelength of 0.95 cm, cannot be stated at the present time. However, if all the droplets in the cloud are less than 300 μm diameter the restriction on droplet size is more than adequately met and it is probably adequately met if all droplets are less than 1 mm diameter. For a Marshall-

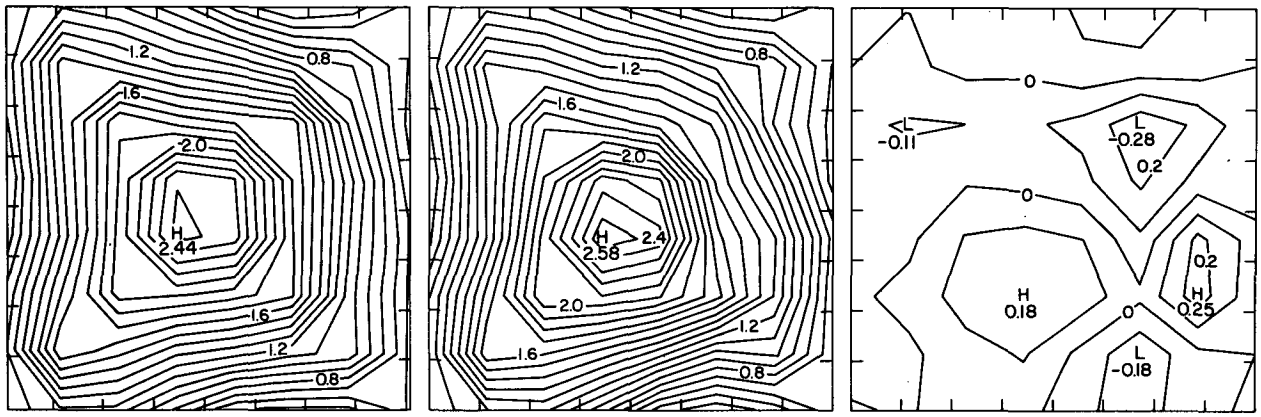

FIG. 7. Original field (left), reconstructed field (center) and error field (right) for a cloud in the environment shown in Fig. 6 on which the fluctuations described in Table 3 are superimposed. The contours are of liquid water in g m^{-3}. Maximum values are shown in their position of occurrence. The rms error is 0.09 g m^{-3}.

TABLE 5. Retrieval of a simulated cloud embedded in an environment with known $\bar{T}$ and $\bar{\rho}_v$ profiles but without knowledge of the cloud's position or the magnitude of the fluctuations of temperature and water vapor superimposed on the means.

Assumed distribution of liquid water ($g\ m^{-3}$)

0.00	0.00	0.00	0.00	0.00	0.00	0.00	0.00	0.00	0.00	0.00	0.00	0.00	0.00	0.00	0.00
0.00	0.00	0.00	0.00	0.00	0.00	0.00	0.00	0.00	0.00	0.00	0.00	0.00	0.00	0.00	0.00
0.00	0.00	0.00	0.00	0.00	0.00	0.00	0.00	0.00	0.00	0.00	0.00	0.00	0.00	0.00	0.00
0.00	0.00	0.00	0.00	0.00	0.00	0.00	0.00	0.00	0.00	0.00	0.00	0.00	0.00	0.00	0.00
0.00	0.00	0.00	0.00	0.62	0.62	0.62	0.62	0.62	0.62	0.62	0.62	0.00	0.00	0.00	0.00
0.00	0.00	0.00	0.00	0.62	1.25	1.25	1.25	1.25	1.25	1.25	0.62	0.00	0.00	0.00	0.00
0.00	0.00	0.00	0.00	0.62	1.25	1.87	1.87	1.87	1.87	1.25	0.62	0.00	0.00	0.00	0.00
0.00	0.00	0.00	0.00	0.62	1.25	1.87	2.50	2.50	1.87	1.25	0.62	0.00	0.00	0.00	0.00
0.00	0.00	0.00	0.00	0.62	1.25	1.87	2.50	2.50	1.87	1.25	0.62	0.00	0.00	0.00	0.00
0.00	0.00	0.00	0.00	0.62	1.25	1.87	1.87	1.87	1.87	1.25	0.62	0.00	0.00	0.00	0.00
0.00	0.00	0.00	0.00	0.62	1.25	1.25	1.25	1.25	1.25	1.25	0.62	0.00	0.00	0.00	0.00
0.00	0.00	0.00	0.00	0.62	0.62	0.62	0.62	0.62	0.62	0.62	0.62	0.00	0.00	0.00	0.00
0.00	0.00	0.00	0.00	0.00	0.00	0.00	0.00	0.00	0.00	0.00	0.00	0.00	0.00	0.00	0.00
0.00	0.00	0.00	0.00	0.00	0.00	0.00	0.00	0.00	0.00	0.00	0.00	0.00	0.00	0.00	0.00
0.00	0.00	0.00	0.00	0.00	0.00	0.00	0.00	0.00	0.00	0.00	0.00	0.00	0.00	0.00	0.00
0.00	0.00	0.00	0.00	0.00	0.00	0.00	0.00	0.00	0.00	0.00	0.00	0.00	0.00	0.00	0.00

Reconstruction from calculated emission data ($g\ m^{-3}$)

0.00	0.00	0.00	0.00	0.00	0.00	0.01	0.00	0.00	0.01	0.00	0.00	0.00	0.00	0.00	0.00
0.00	0.00	0.00	0.00	0.00	0.02	0.08	0.11	0.11	0.10	0.03	0.00	0.00	0.00	0.00	0.00
0.00	0.00	0.00	0.00	0.00	0.02	0.08	0.15	0.17	0.14	0.02	0.00	0.00	0.00	0.00	0.00
0.00	0.00	0.00	0.00	0.00	0.00	0.00	0.13	0.11	0.07	0.00	0.00	0.00	0.00	0.00	0.00
0.00	0.00	0.00	0.00	0.58	0.61	0.57	0.69	0.60	0.56	0.55	0.57	0.00	0.00	0.00	0.00
0.00	0.00	0.00	0.00	0.57	1.26	1.15	1.40	1.28	1.20	1.21	0.59	0.00	0.00	0.00	0.00
0.00	0.00	0.00	0.00	0.51	1.09	1.65	1.99	1.83	1.72	1.05	0.46	0.00	0.00	0.00	0.00
0.00	0.00	0.00	0.02	0.50	1.11	1.77	2.67	2.49	1.78	1.05	0.45	0.00	0.00	0.00	0.00
0.00	0.00	0.00	0.02	0.55	1.14	1.86	2.68	2.54	1.90	1.19	0.59	0.03	0.00	0.00	0.00
0.00	0.00	0.00	0.00	0.52	1.18	1.90	2.04	2.01	1.90	1.20	0.62	0.02	0.00	0.00	0.00
0.00	0.00	0.00	0.01	0.64	1.29	1.36	1.30	1.31	1.27	1.24	0.62	0.01	0.01	0.00	0.00
0.00	0.00	0.00	0.00	0.64	0.61	0.62	0.59	0.62	0.63	0.62	0.61	0.00	0.00	0.00	0.00
0.00	0.00	0.00	0.00	0.02	0.01	0.03	0.00	0.00	0.01	0.02	0.01	0.01	0.02	0.00	0.00
0.00	0.00	0.00	0.00	0.00	0.00	0.00	0.03	0.01	0.04	0.02	0.00	0.00	0.00	0.00	0.00
0.00	0.00	0.00	0.00	0.00	0.00	0.00	0.00	0.00	0.00	0.00	0.00	0.00	0.00	0.00	0.00
0.00	0.00	0.00	0.00	0.00	0.00	0.00	0.00	0.00	0.00	0.00	0.00	0.00	0.00	0.00	0.00

Palmer drop size distribution, drizzle at 0.2 mm h^{-1} has 70% of the rainwater in drops < 1 mm diameter and 90% in drops < 1.25 mm diameter, light rain at 1 mm h^{-1} has 45% of the water in drops < 1 mm and 55% in drops < 1.25 mm, whilst moderate rain at 10 mm h^{-1} has only 15% of its water in drops < 1 mm diameter. Hence, whilst the technique should be capable of determining liquid water content in clouds producing only drizzle or very light rain it will not be useful when the rain rate is significantly higher. It is therefore likely to be of value only in the early stages of cloud development before significant precipitation develops.

When ice particles fall through the 0°C level and develop a wet surface they will absorb and may scatter microwave radiation to a greater degree than before and emission from them may exceed that of water droplets of equivalent size. Since such melting ice particles are likely to exceed 1 mm in size the emission will also depend upon their size distribution and not just the quantity of water present. Radiometric techniques are not capable of yielding the liquid water content of the clouds in these conditions.

It is necessary to know the environmental temperature and water vapor mixing ratio as well as that within the cloud to be able to retrieve the cloud liquid water distribution by the inversion technique proposed. However, it appears from the simulation studies that the accuracy with which these quantities needs to be known is not very high, being well within the limits which would be available from a nearby radiosonde or research aircraft sounding. Cloud temperature and water vapor mixing ratio are probably not known from such soundings. However, unless vertical velocities are very large, the cloud air is not likely to differ in temperature from that of the environment by more than

1°C. Further, if small droplets are present—which will be the case in the pre-precipitation phase of cloud development—supersaturations or subsaturations will be small (well under 5%) and the vapor mixing ratio will hence be very close to the saturation mixing ratio at the cloud temperature, i.e., the environmental air temperature. It is possible that a more accurate knowledge of water vapor concentration would improve the accuracy with which liquid water could be retrieved from the radiometric measurements. If this proves to be the case (and it will be investigated in later simulation studies) it is possible that a dual-channel radiometer, with the second channel in an absorption band for water vapor, could give useful additional information.

7. Conclusions

As a result of a series of computer simulations it appears that the distribution of liquid water throughout a vertical section of a cloud positioned between two scanning radiometers can be determined by inversion of the emission at a wavelength of about 1 cm received by the radiometers. The rms error in the reconstructed field is about 10% of the maximum value of liquid water concentration present in the cloud and the spatial resolution of the technique is of the order of a few hundred meters. Since the emission from the liquid water is temperature-dependent and water vapor in the cloud and its environment also emits, though less strongly at a suitable wavelength than the liquid water, it is necessary to know the mean vertical profiles of temperature and mixing ratio. However, these parameters need not be known to high accuracy and information from a nearby radiosonde or from a research aircraft sounding is adequate. Since the temperature in a cloud is unlikely to differ by more than 1°C from its environment and the air is almost certainly within a few percent of saturation an environmental sounding is adequate to define conditions in the cloud.

At centimeter wavelengths ice emits very much less than an equal mass of water at the same temperature so the technique measures the liquid only, not the ice. However, melting ice particles will have a film of water on their surface and will emit much more strongly.

The method is only capable of yielding the liquid water content provided most of the water is in drops which are small compared to the wavelength, i.e., for a wavelength of 1 cm they must be less than 1 mm diameter. This restricts the technique to the pre-precipitation phase of cloud development or at least to conditions where the rain rate is less than about 1 mm h^{-1}.

The need to integrate the low intensity emissions from the cloud limits the maximum rate at which the cloud can be scanned. In practice a period of 2–3 minutes is likely to be necessary. Hence the method would not be satisfactory if the cloud were undergoing rapid evolution or if it were moving rapidly relative to the radiometers. In most circumstances this is not likely to be a serious problem.

By scanning in planes away from the zenith it would be possible to build up a three-dimensional picture of the liquid water distribution throughout a cloud. The main limitation here would be the extra time required and hence the greater need for stationarity.

Acknowledgments. It is a pleasure to acknowledge the useful discussions and comments of Drs. D. C. Hogg and J. B. Snider of the Wave Propagation Laboratory/NOAA. Dr. S. Twomey of the University of Arizona contributed useful suggestions on the inversion procedure.

APPENDIX

Formulae for Absorption

The formulae for κ_l and α_v from Westwater (1972) are

$$1)\quad \kappa_l = \frac{1.885 \times 10^{-3}}{\lambda} I\left(\frac{1-\epsilon}{2+\epsilon}\right) \quad [\mathrm{m}^{-1}(\mathrm{g\ m}^{-3})^{-1}]$$

where

$$\epsilon = \epsilon_\infty + \frac{\epsilon_0 - \epsilon_\infty}{1 + i\left(\frac{\lambda_s}{\lambda}\right)^{1-\gamma}}$$

λ = 0.947 cm (wavelength corresponding to 31.65 GHz)
ϵ_∞ = 4.5
$\epsilon_0 = -29.62 + 32155.45/T$
$\log_{10}\lambda_s = -2.9014 + 921.0935/T$
γ = 0.02
T = temperature (K)
$I(\ )$ = the imaginary part of the complex variable.

$$2)\quad \alpha_v = \rho_v\left(\frac{318}{T}\right)^{5/2} \tilde{\nu}^2 C_1 \beta \left[\frac{1}{(\tilde{\nu}-\tilde{\nu}_v)^2+\beta^2} + \frac{1}{(\tilde{\nu}+\tilde{\nu}_v)^2+\beta^2}\right] \exp(2.025 - 644/T) + 318 C_2 \tilde{\nu}^2 \beta / T \quad (\mathrm{m}^{-1})$$

where

$\tilde{\nu} = 1/\lambda$ cm^{-1}
$\tilde{\nu}_v$ = 0.7417 cm^{-1}
$C_1 = 8.312 \times 10^{-7}$
$C_2 = 1.402 \times 10^{-5}$

$$\beta = \left(\frac{P}{1013.25}\right)\left(\frac{318}{T}\right)^{0.625} \beta_1(1 + \beta_2 \rho_v)$$

P = pressure (mb)

$\beta_1 = 0.08478$
$\beta_2 = 7.08 \times 10^{-3}$.

The formula for α_{02} from Falcone (1966) is

$$\alpha_{02} = \frac{C_3 \rho_{02} \mu}{T\lambda^2}\left[\frac{1}{\tilde{\nu}^2 + \mu^2} + \frac{1}{(\tilde{\nu} - \tilde{\nu}_{02})^2 + \mu^2} + \frac{1}{(\tilde{\nu} + \tilde{\nu}_{02})^2 + \mu^2}\right] (\mathrm{m}^{-1})$$

where

$C_3 = 3.58 \times 10^{-5}/\log_{10} e$
ρ_{02} = oxygen density (g m^{-3})
$\mu = 3.146 \times 10^{-3}\, PT^{-0.85}$
$\tilde{\nu}_{02} = 2$ (cm^{-1}).

REFERENCES

Falcone, V., 1966: Calculations of apparent sky temperature at millimeter wavelengths. *Radio Sci.*, **1**(new series), 1205–1209.

Hanson, R. J., and K. Haskell, 1982: Two algorithms for the linearly constrained least squares problem. *ACM Trans. Math. Soft.*, **8**, 323–333.

Herman, G. T., 1980: *Image Reconstruction from Projections—The Fundamentals of Computerized Tomography.* Academic Press, 316 pp.

Hogg, D. C., F. O. Guiraud, J. B. Snider, M. T. Decker and E. R. Westwater, 1983: A steerable dual-channel microwave radiometer for measurement of water vapor and liquid in the troposphere. *J. Climate Appl. Meteor.*, **22**, 789–806.

Lawson, C. L., and R. J. Hanson, 1974: *Solving Least Squares Problems.* Prentice-Hall, 340 pp.

Shaari, W. A., and D. B. Hodge, 1978: Microwave radiometric detection of rain cells using tomography. The Ohio State University Electro Science Laboratory Tech. Note No. 9, 119 pp.

Westwater, E. R., 1972: Microwave emission from clouds. NOAA Tech. Rep. ERL 219-WPL 18, 43 pp.